

O. Bokhove  
Department of Applied Mathematics  
University of Twente  
P.O. Box 217  
Enschede, The Netherlands  
o.bokhove@math.utwente.nl

Peter Lynch  
Meteorology and Climate Centre  
School of Mathematical Sciences  
University College Dublin  
Dublin, Ireland  
peter.lynch@ucd.ie

# Air parcels and air particles: Hamiltonian dynamics

**We present a simple Hamiltonian formulation of the Euler equations for fluid flow in the Lagrangian framework. In contrast to the conventional formulation, which involves coupled partial differential equations, our “innovative” mathematical formulation involves only ordinary differential equations coupled by integral equations. We illustrate the utility of the new formulation by applying it to a simple stability problem for the atmosphere.**

A novel and simple formulation of the Euler equations for fluid flow will be derived in this paper. We consider the dynamics of (dry) air, modelling it as an ideal gas. In reality, the continuum nature of air is lost at sufficiently small, molecular scales: the thermodynamics of an air parcel in the usual macroscopic continuum model results from an averaging over the rapidly moving molecules.

A *parcel of air* is a coherent piece of air carried along by the wind. It is large enough to contain many molecules, but small enough that we may assume bulk fluid properties uniform throughout it. The concept of an air parcel was introduced by Richardson (1922) in his discussion of radiation in the atmosphere, and has become part of the everyday language of meteorologists, especially in the context of the stability of vertical motions. We can visualize air parcel flow by following the motion of a *tracer*. For example, on a sunny day, air parcel movement becomes visible through the swirling motion of dust particles in the air. Similarly, smoke particles from a cigarette or smoke stack depict the approximate air parcel motion.

Neither the dust nor the smoke particles are infinitesimal and thus do not correspond precisely to an air parcel, but they serve as good approximations for flow scales much larger than the particle size. Note that a *particle* is a discrete entity, whereas a *parcel* is a continuum entity. We will later discuss a numerical discretization of air parcels in which parcels are discretized by particles.

We could also visualize air parcel flow by marking a parcel with a coloured dye. Were each parcel to have a unique colour, the parcels would be individually tagged or *labelled*. We denote the continuum labels of air parcels by  $\mathbf{a}$ . For flow in three dimensions,  $\mathbf{a} = (a_1, a_2, a_3)^T$  is a three-dimensional (3D) column vector in Cartesian label coordinates, where  $(\cdot)^T$  denotes the transpose.

There are two fundamentally different frameworks for the study of fluid flow. In the Lagrangian framework, we focus on individual parcels of fluid, identified by labels as described above. To study the dynamics, we follow the evolution of the individual parcels as they are carried along by the flow.

The position of a particular parcel is denoted by  $\chi(\mathbf{a}, t)$ , a time-varying vector in three-dimensional space. Fluid properties are then functions of  $\mathbf{a}$  and time  $t$ . In the Eulerian framework, we use a reference frame fixed in space and watch the evolution of the flow as it passes a fixed location. We denote this position by  $\mathbf{x} = (x, y, z)^T$ , a vector fixed in three-dimensional space. Fluid properties are then functions of  $\mathbf{x}$  and of time  $t$ . The map  $\mathbf{a} \mapsto \chi(\mathbf{a}, t)$  relates the label coordinates  $\mathbf{a}$  to the position coordinates  $\mathbf{x}$  expressing that the parcel with label coordinate  $\mathbf{a}$  resides at the location  $\mathbf{x} = \chi(\mathbf{a}, t)$  at time  $t$ .

The local thermodynamic state at parcel location  $\mathbf{x} = \chi(\mathbf{a}, t)$  is determined by two of the following four variables: density  $\rho(\mathbf{x}, t)$ , potential temperature  $\theta(\mathbf{x}, t)$  (a standard quantity in meteorology and a monotonic and invertible function of the entropy), pressure  $p(\mathbf{x}, t)$  and temperature  $T(\mathbf{x}, t)$ . The remaining two variables follow from the relationships valid for an ideal gas (see Appendix Box 1).

Classically, air motion is governed by the compressible Navier-Stokes equations including a continuity equation (expressing mass conservation) and an equation of state such as the ideal gas law. The full Navier-Stokes equations include the effect of fluid viscosity or friction, and forcing. For large scale applications in meteorology, it is common

to consider inviscid (frictionless) dynamics of air motion, but to retain all the complicated and essential nonlinearities. Furthermore, in numerical weather and climate prediction, a closure problem arises due to the discretization: unresolved gravity-wave motion, quasi-2D turbulence, and 3D turbulence (in decreasing order of importance) require an accurate representation of their effect on the larger, resolved scales of motion. Scales associated with these physical processes are still much larger than the viscous, molecular scales. We therefore consider below the unforced, inviscid Navier-Stokes equations, that is, the compressible Euler equations for an ideal gas.

The position of an air parcel in 3D space is a vector  $\chi(\mathbf{a}, t)$  depending on the label  $\mathbf{a}$  and the time  $t$  as the air parcel moves through space over time. An air parcel with position  $\chi(\mathbf{a}, t)$  has a (Lagrangian) velocity

$$(1) \quad \dot{\chi}(\mathbf{a}, t) = \frac{\partial \chi(\mathbf{a}, t)}{\partial t} = \mathbf{u}(\chi(\mathbf{a}, t), t).$$

The partial derivative  $\partial/\partial t$  here implies a variation of  $t$  while keeping the parcel label  $\mathbf{a}$  fixed, and  $\mathbf{u}(\mathbf{x}, t)$  is the (Eulerian) velocity at a fixed location  $\mathbf{x}$  in space. The term *Lagrangian* implies that we are moving with the flow and the independent coordinates are time  $t$  and label coordinates  $\mathbf{a}$  when we consider air as a continuum of air parcels. Similarly, the term *Eulerian* implies that the independent coordinates are the fixed spatial coordinates  $\mathbf{x}$  and the time  $t$ .

The compressible Euler equations are usually expressed as partial differential equations (PDE's) and an algebraic equation of state. In the Eulerian framework, the partial derivatives are taken with respect to  $\mathbf{x}$  and  $t$ , and the observer remains at a fixed point in space. In the Lagrangian framework, the partial derivatives are taken with respect to labels  $\mathbf{a}$  and time  $t$ , and the observer moves with the fluid flow.

The PDE's can be derived succinctly from Hamiltonian formulations involving (generalized) Poisson brackets for an arbitrary functional and a Hamiltonian or energy functional. These functionals are either integrals over the Lagrangian 3D label space  $\mathbf{a}$ , or over the fixed Eulerian space  $\mathbf{x}$ . They depend on either the fields  $\chi(\mathbf{a}, t)$  and  $\dot{\chi}(\mathbf{a}, t)$  (Lagrangian viewpoint), or the velocity  $\mathbf{u}(\mathbf{x}, t)$ , density  $\rho(\mathbf{x}, t)$  and potential temperature  $\theta(\mathbf{x}, t)$  (Eulerian viewpoint). This Hamiltonian structure of the Euler equations is of interest because it relates immediately to various constants of motion and associated flux conservation laws. Unfortunately, this structure involves PDE's and functionals, and is *much* more complicated than the standard Hamiltonian theory, which involves ordinary differential equations (ODE's).

The novel Hamiltonian treatment of the parcel dynamics of the Euler equations that we will present below involves only ODE's and integral equations. It turns out to be much simpler than the usual treatment, and can be transformed to the usual Hamiltonian description of the

dynamics in terms of PDE's in the most straightforward way we know. For simplicity of presentation, we confine attention to one spatial dimension. However, the approach is easily generalized.

A key notion in what follows is the realization that the dynamics of a distinguished fluid parcel, singled out, is governed by a single ODE, a non-autonomous Hamiltonian finite-dimensional system. Consider now a specific or distinguished air parcel, labelled with (vector) label  $\mathbf{A}$ , amongst the continuum of air parcels  $\mathbf{a}$ . Thus, we write the position of the distinguished air parcel  $\mathbf{A}$  in particular by  $\mathbf{X} = \mathbf{X}(t) = \chi(\mathbf{A}, t)$ . It is a function of time, not a function of  $\mathbf{A}$ , although we could indicate its parametric dependence on  $\mathbf{A}$  by writing  $\mathbf{X} = \mathbf{X}(t; \mathbf{A})$ . The velocity of the distinguished air parcel  $\mathbf{A}$  is denoted by  $\mathbf{U} = \mathbf{U}(t; \mathbf{A}) = \mathbf{u}(\chi(\mathbf{A}, t), t)$ ; cf. (1).

### 1. Hamiltonian parcel dynamics

Recently, developments in Hamiltonian numerical particle methods for atmospheric dynamics have led to a novel Hamiltonian description of the compressible Euler equations for air (Bokhove and Oliver 2006). This consists of Hamiltonian ODE's, one for each distinguished air parcel with Hamiltonian  $H = H(t)$  in isolation, and an integral equation binding the continuum of air parcels together. As stated above, we consider the case of one space dimension,  $z$  the vertical coordinate, normal to the Earth's surface at a certain latitude and longitude. Let  $Z(t)$  be the vertical position of a distinguished parcel  $A$ , and  $W(t)$  its velocity in the vertical direction. The dynamics of the parcel will be described in a canonical Hamiltonian formalism as if it were an isolated particle.

We start therefore with the Hamiltonian dynamics of a particle, or of one specific air parcel, in a potential  $V(z, t)$ ; it is given by

$$(2a) \quad \frac{dZ}{dt} = \frac{\partial H_v}{\partial W} = W$$

$$(2b) \quad \frac{dW}{dt} = -\frac{\partial H_v}{\partial Z} = -\frac{\partial V}{\partial Z}$$

(see, e.g., Arrowsmith and Place 1992). The Hamiltonian  $H_v$  comprises the sum of the kinetic and potential energy

$$(3) \quad H_v = H_v(Z, W, t) = \frac{1}{2}W^2 + V(Z, t),$$

where the potential must have the same physical dimensions as  $W^2/2$ . For a time-independent potential  $V = V(Z)$  the Hamiltonian is a constant of motion:

$$(4) \quad \frac{dH_v}{dt} = \frac{\partial H_v}{\partial Z} \frac{dZ}{dt} + \frac{\partial H_v}{\partial W} \frac{dW}{dt} = 0.$$

If  $V(Z, t)$  depends explicitly on time, then the energy is no longer constant:  $dH_v/dt = \partial V/\partial t \neq 0$ .

For what choice of the potential  $V(Z, t)$  do we obtain the compressible Euler equations of motion for the atmosphere? It turns out (by inspection, see Bokhove and Oliver 2006) that the appropriate choice is to take  $V$  equal

to the Montgomery potential

$$(5) \quad \begin{aligned} M = M(p(Z, t), Z) &= \Theta \Pi_e + g Z \\ &= c_p \Theta (p(Z, t)/p_r)^\kappa + g Z \end{aligned}$$

where  $\Theta = \Theta(t)$  is the potential temperature and  $\Pi_e = \Pi_e(Z, t)$  is Exner's function defined by  $\Pi_e = c_p (p(Z, t)/p_r)^\kappa$  with the Eulerian pressure  $p = p(z, t)$  evaluated at the parcel's position  $z = Z(t)$ . The reference pressure  $p_r \approx 1000\text{mb}$ , specific heat  $c_p \approx 1004\text{J}/(\text{kg K})$  at fixed pressure,  $\kappa = R/c_p$  and acceleration of gravity  $g$  are all constant (see Appendix Box 1). Potential temperature  $\Theta = \Theta(t)$  is a thermodynamic variable and a constant of motion, independent of  $Z$ , following the air parcel  $A$ , such that  $d\Theta/dt = 0$ , under the assumed adiabatic and inviscid conditions. We note from the units given that Montgomery potential  $M$  has the same physical dimension as  $W^2/2$ .

## 2. Catch-22: where is the continuum?

Substitution of the Montgomery potential  $M$  in (5) for the potential  $V$  in (2), made explicit by denoting  $H_v$  by  $H_c$ , yields the Lagrangian form of the compressible Euler equations of motion for a particular air parcel:

$$(6a) \quad \frac{dZ}{dt} = \frac{\partial H_c}{\partial W} = W,$$

$$(6b) \quad \frac{dW}{dt} = -\frac{\partial H_c}{\partial Z} = -\Theta \frac{\partial \Pi_e}{\partial Z} - g,$$

$$(6c) \quad \frac{d\Theta}{dt} = 0$$

with Hamiltonian

$$(7) \quad \begin{aligned} H_c(Z, W, \Theta, t) &= \frac{1}{2}W^2 + \Theta \Pi_e(p(Z, t)) + g Z \\ &= \frac{1}{2}W^2 + c_p \Theta (p(Z, t)/p_r)^\kappa + g Z. \end{aligned}$$

**Exercise:** Verify the expressions in the dynamics (6) by using the Hamiltonian (7).  $\square$

However, there seems to be a Catch-22 in the dynamics (6)–(7) for the continuum of labels! First, when initial conditions  $Z(0) = Z(0; A)$  and  $W(0) = W(0; A)$  are provided for all labels  $A$ , the continuum motion of all air parcels can be calculated from the ordinary differential equations (6)–(7). A natural choice is  $Z(0; A) = A$ . Additionally, in the momentum equation (6b), the Eulerian pressure  $p(z, t)$  must be evaluated at the parcel position  $z = Z(t)$ , yet the pressure in turn depends on the continuum of air parcels as well. In other words, the system is not closed unless we specify or calculate the pressure  $p(z, t)$ . We write the pressure  $p(z, t)$  as an Eulerian function of fixed vertical coordinate  $z$  and time  $t$  yet we will evaluate it at the position  $Z(t) = Z(t; A)$  of the distinguished parcel  $A$ .

The pressure can be specified or calculated in several ways; we will consider three different possibilities. *First*, we can take an exact (steady state) solution of the Euler equations, written as a system of PDE's, to investigate the associated parcel motion. The problem then merely shifts to the question: how do we find an exact solution

of the equations? Nevertheless, when we have an exact expression for  $p(z, t)$  we can explore the associated parcel motion. *Second*, observations of pressure at discrete points in space-time can be used to reconstruct  $p(z, t)$ . *Third*, we can close the Hamiltonian system (6)–(7) by calculating the pressure explicitly.

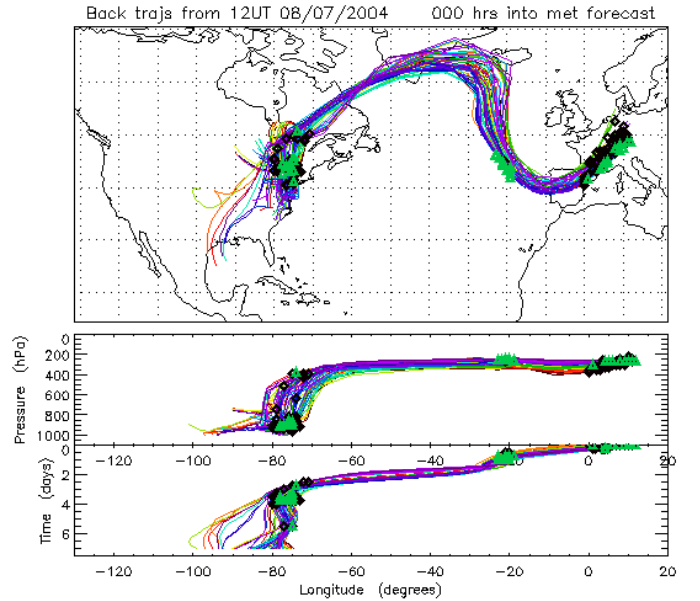


Fig. 1. Particles are released in Europe and the backwards trajectories are calculated using the wind velocity backwards in time. Intercontinental Transport of Ozone and Precursors (ITOP) project: picture courtesy <http://badc.nerc.ac.uk/data/itop/>

The first two options are akin to kinematic studies of fluid motion, in which the motion of particles is studied given a wind field  $\mathbf{u}(z, t)$  in 3D, to be evaluated for a finite number of parcel positions  $\mathbf{X}_i$  with  $i = 1, \dots, N$  and  $N$  the number of particles used. Such kinematic studies are important in forecasts of pollutant spreading. They lead to the spaghetti diagrams in Fig. 1, where passive pollutant particles or tracers are released over Europe and their trajectories traced backwards in time using the wind field. Their spread is subsequently monitored. Instead of a (vector) wind field, our Hamiltonian formalism needs only a (scalar) pressure field to compute the movement of a discrete number of particles in a numerical study. In more than one dimension, less information is thus required and the strategy is more dynamic, although the pressure requires specification, and frictional and forcing effects have been excluded. In Fig. 2 we show a collection of Lagrangian trajectories for air parcels originating at different times and levels. The convoluted nature of the trajectories illustrates the complexity of nonlinear atmospheric flow. It would be interesting to compare these two

strategies to calculate particle motion in this meteorological context, to assess the relevance of the extra dynamic structure provided in the parcel Hamiltonian approach<sup>1</sup>. Spurious agglomeration of particles can then be avoided since the flow is symplectic, and thus volume preserving. Furthermore, these properties can be preserved with symplectic numerical techniques.

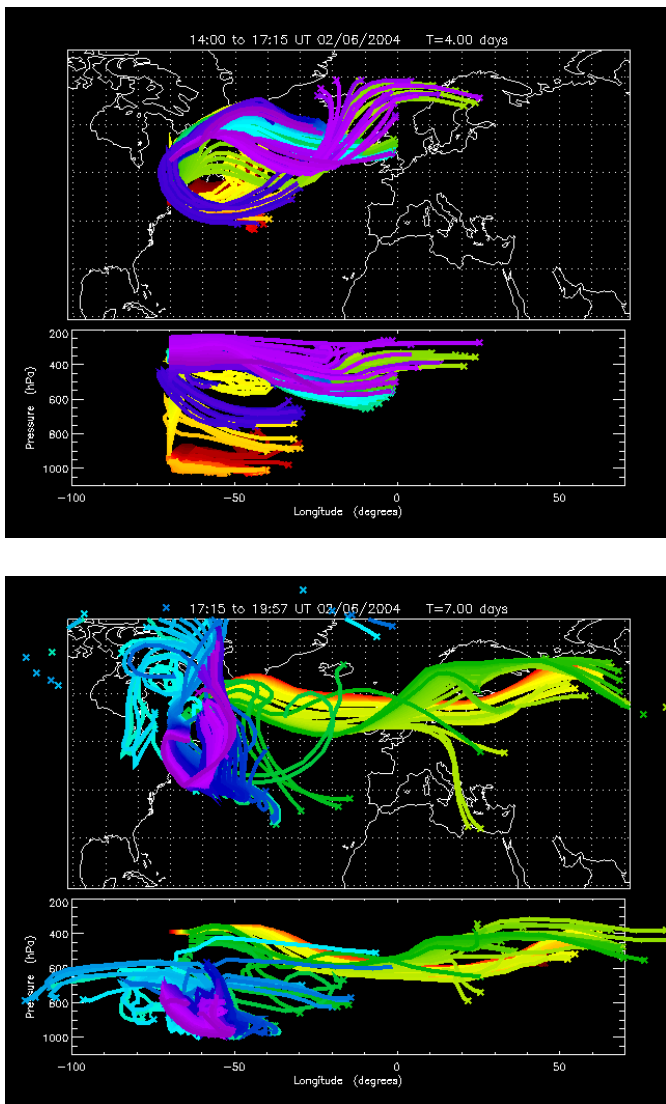


Fig. 2 Trajectories of air parcels released at several levels over a period of hours. The evolution of two sets of trajectories is shown in latitude-longitude and pressure-longitude plots. The points of release are shown with crosses. The goal of the ITOP programme is to study intercontinental transport of pollutants (see <http://badc.nerc.ac.uk/data/itop/>). The motivation is that Eulerian, point measurements of photochemical processes are less accurate than measurements along Lagrangian (5-day) trajectories. Thanks to John Methven (University of Reading) for images [7].

For the third option, closure of the Hamiltonian system (6)–(7) by calculation of the pressure, we require Eulerian expressions for the density  $\rho(z, t)$  and Eulerian potential temperature  $\theta(z, t)$ , because

$$(8) \quad p(z, t) = p(\rho(z, t), \theta(z, t)) = \left( \frac{p_r^\kappa}{R \rho(z, t) \theta(z, t)} \right)^{\frac{1}{\kappa-1}}$$

with constants  $p_r, \kappa$  and  $R$ ; see Appendix Box 1.

The map  $a \mapsto \chi(a, t)$  relates the label coordinates  $a$  to the vertical coordinate  $z$  such that  $z = \chi(a, t)$ . The density  $\rho(z, t)$  and the mass-weighted potential temperature  $\rho(z, t) \theta(z, t)$  required in (8) are determined by linking them to the Jacobian between label space  $a$  and Eulerian space  $z$ . In addition, the potential temperature satisfies

$$(9) \quad \Theta(t) = \Theta(t; A) = \theta(Z(t; A), t),$$

and on a distinguished parcel  $A$  it is constant  $\Theta(t; A) = \Theta_0(A)$  as we saw earlier that  $d\Theta/dt = 0$ . An element of mass  $dm$  is by definition density times volume, and we therefore find

$$(10) \quad dm = \rho(z, t) \Delta x \Delta y dz = \rho_0(a) \Delta b \Delta c da,$$

where  $\Delta x, \Delta y, \Delta b$  and  $\Delta c$  are unity, so that the density  $\rho$  retains its usual interpretation as mass/volume in this one-dimensional case. Here  $b$  and  $c$  are the labels in the  $x$  and  $y$  directions. Furthermore, the mass  $dm$  is conserved for labels between  $a$  and  $a + da$  with a label-weighted density  $\rho_0(a)$ . With the ‘natural’ choice, where the labels initially coincide with the coordinate values, such that  $z = \chi(a, 0) = a$ , we thus find  $\rho(z, 0) = \rho_0(a)$  initially. The consequence of (10) is that

$$(11) \quad \frac{\rho_0}{\rho(\chi(a, t), t)} = \frac{\partial \chi(a, t)}{\partial a}$$

is the Jacobian between the label space with label  $a$  and Eulerian space with coordinate  $z = \chi(a, t)$ . The trick now is to rewrite the density-weighted potential temperature  $\rho(z, t) \theta(z, t)$  as an integral over label space by using the delta function  $\delta(z - z')$  with dummy coordinate  $z'$  and the Jacobian (11). By using (9) and (11) with  $z' = \chi(a, t)$ , we obtain the following

$$(12) \quad \begin{aligned} \rho(z, t) \theta(z, t) &= \int_0^h \rho(z', t) \theta(z', t) \delta(z - z') dz' \\ &= \int_0^{A_h} \rho(\chi(a, t), t) \Theta_0(a) \delta(z - \chi(a, t)) \frac{\partial \chi(a, t)}{\partial a} da \\ &= \int_0^{A_h} \rho_0(A) \Theta_0(A) \delta(z - Z(t; A)) dA, \end{aligned}$$

where  $\Theta(t; A) = \Theta(0; A) = \Theta_0(A)$  is conserved following an air parcel and  $h = z(A_h, t)$  in a domain  $z = [0, h]$  in which  $A_h$  is the air parcel label at the top of our one-dimensional atmosphere. The label coordinates  $a$  and  $A$  in the last two integrals of (12) are dummies in the integration. We have therefore passed without problems from the

<sup>1</sup>We proposed this as a bachelor project in Twente.

general label coordinates  $a$  to the distinguished labels  $A$ , with the corresponding change  $\chi(A, t) = Z(t; A) = Z(t)$ . We assume there is a solid boundary at  $z = 0$  such that the parcel initially at the boundary never leaves  $z = 0$  as its vertical velocity remains zero. Likewise, the density satisfies

$$(13) \quad \begin{aligned} \rho(z, t) &= \int_0^h \rho(z', t) \delta(z - z') dz' \\ &= \int_0^{A_h} \rho_0(A) \delta(z - Z(t; A)) dA. \end{aligned}$$

The usual equation expressing conservation of mass

$$(14) \quad \partial_t \rho + \partial_z(\rho w) = 0,$$

with  $\rho(z, t)$  and  $w(z, t)$ , is obtained by taking the time derivative of (13) while using (6a). Likewise, conservation of density-weighted potential temperature

$$(15) \quad \partial_t(\rho\theta) + \partial_z(\rho\theta w) = 0,$$

with also  $\theta(z, t)$ , is obtained with the use of (6a) and (6c). Partial derivatives  $\partial_t = \partial/\partial t$  and  $\partial_z = \partial/\partial z$  are used here with  $z$  and  $t$  constant, respectively, and with dependent variables  $w(z, t)$ ,  $\rho(z, t)$  and  $\theta(z, t)$ . Note that the Eulerian velocity  $w(z, t)$  is used, and recall that its relation with the Lagrangian velocity  $W(t)$  for the special parcel  $A$  at position  $z = Z(t)$  is  $W(t; A) = w(Z(t; A), t)$ .

In summary, the compressible Euler equations of motion for air modelled as an ideal gas are governed by the parcel Hamiltonian system (6)–(7) with a continuum infinity of initial conditions, one for each distinguished air parcel, the pressure  $p(z, t)$  defined by (8) in terms of the product of density and potential temperature, which is, in turn, provided by the integral (12) over all labels. Density can be recovered separately via (13).

Bound together the dynamics of air is then governed by the following closed system of equations:  $\forall A$  in  $Z = Z(t; A)$ ,  $W = W(t; A)$  and  $\Theta = \Theta(t; A)$  the dynamics is

$$(16a) \quad \frac{dZ}{dt} = \frac{\partial H_c}{\partial W} = W,$$

$$(16b) \quad \frac{dW}{dt} = -\frac{\partial H_c}{\partial Z} = -c_p \Theta \frac{\partial (p(Z, t)/p_r)^\kappa}{\partial Z} - g,$$

$$(16c) \quad \frac{d\Theta}{dt} = 0,$$

$$(16d) \quad H_c(Z, W, \Theta, t) = \frac{1}{2}W^2 + c_p \Theta (p(Z, t)/p_r)^\kappa + gZ$$

with initial conditions  $\Theta(0; A) = \Theta_0(A)$ ,  $Z(0; A) = A$ ,  $W(0; A) = W_0(A)$  and  $\rho_0(A) = \rho(Z(0; A) = A, 0)$ ; and, furthermore

$$(17a) \quad p(Z, t) = \left( \frac{p_r^\kappa}{R \rho(Z, t) \theta(Z, t)} \right)^{1/(\kappa-1)}$$

$$(17b) \quad \rho(Z, t) \theta(Z, t) = \int_0^{A_h} \rho_0(\tilde{A}) \Theta_0(\tilde{A}) \delta(Z - Z'(t; \tilde{A})) d\tilde{A}.$$

Note the dummy integration label  $\tilde{A}$  in (17b) as opposed to the distinguished label  $A$  in  $Z = Z(t; A)$ .

### 3. Generalized Poisson brackets

We summarize the Hamiltonian parcel formulation (16)–(17) succinctly as

$$(18) \quad \frac{dF}{dt} = \{F, H_c\} \text{ with } \{F, G\} \equiv \frac{\partial F}{\partial Z} \frac{\partial G}{\partial W} - \frac{\partial F}{\partial W} \frac{\partial G}{\partial Z}$$

for Hamiltonian (16d) and arbitrary functions  $F = F(Z, W, \theta, t)$  and  $G = G(Z, W, \theta, t)$ , valid for all fluid labels by specifying the (distinct) initial conditions for each label.

**Exercise:** Show that if we take  $F \in \{Z, W, \Theta\}$  in (18), together with (16d), then we obtain the parcel equations of motion in (16).  $\square$

To close the system, we additionally determine the pressure  $p(z, t)$  in Hamiltonian (16d) through (17). The formulation is Hamiltonian because it satisfies the following properties: the (generalized) Poisson bracket  $\{F, G\}$  in (18) is anti-symmetric:  $\{F, G\} = -\{G, F\}$ , and it satisfies the Jacobi identity

$$(19) \quad \{F, \{G, K\}\} + \{G, \{K, F\}\} + \{K, \{F, G\}\} = 0$$

for arbitrary functions  $F, G$  and  $K$ . These properties are readily proven by inspection and direct manipulation. In three dimensions and for air in our Earthly rotating frame of reference, the generalized Poisson bracket is not canonical as in (18), but it is still Hamiltonian, because the bracket is anti-symmetric and satisfies the Jacobi identity.

The Euler equations in Eulerian form

$$(20a) \quad \partial_t \rho + \partial_z(\rho w) = 0,$$

$$(20b) \quad \partial_t w + w \partial_z w = -\frac{1}{\rho} \frac{\partial p}{\partial z} - g = -\theta \frac{\partial \Pi_e}{\partial z} - g,$$

$$(20c) \quad \partial_t \theta + w \partial_z \theta = 0,$$

are partial differential equations. These equations and their Hamiltonian formulation are readily derived from the parcel Hamiltonian formulation (18) and (16d), with (12) and (13), following the appendix in Bokhove and Oliver (2007), and Bokhove and Oliver (2006) for the 3D case. A cursory comparison between (16) and (20) indicates that  $W(t) \rightarrow w(z, t)$  and  $\Theta(t) \rightarrow \theta(z, t)$ , and that  $d(\cdot)/dt = \partial(\cdot)/\partial t + w(z, t) \partial(\cdot)/\partial z$  is the total or material time derivative following an air parcel. Also note that

$$(21) \quad \frac{1}{\rho} \frac{\partial p}{\partial z} = \frac{\theta \kappa c_p p^{\kappa-1}}{p_r^\kappa} \frac{\partial p}{\partial z} = \theta \frac{\partial \Pi_e}{\partial z}$$

with  $\Pi_e = c_p (p/p_r)^\kappa$  and  $\kappa = R/c_p$ , by using expressions (34) and (37) (in Appendix Box 1).

### 4. Attractions of the Hamiltonian framework

The reasons for our fascination with the parcel Hamiltonian formulation are manifold. The formulation is simpler than the classical formulation, as it is comprised of ODE's and (two) integral relations instead of a system of PDE's. We consider four aspects of this formulation now.

*First*, the derivation of the Hamiltonian formulation of the PDE's involves the transformation of standard function derivatives (involving functions  $F = F(Z, W, \Theta, t)$ ) in

the parcel framework into functional derivatives (involving functionals  $\mathcal{F} = \mathcal{F}(w, \rho, \theta)$ , that is, integrals including the fields  $w(z, t)$ ,  $\rho(z, t)$  and  $\theta(z, t)$ ) in the Eulerian framework.

The Hamiltonian expression of (20) is formally similar to (18),

$$(22) \quad \frac{d\mathcal{F}}{dt} = \{\mathcal{F}, \mathcal{H}\},$$

but with functionals  $\mathcal{F}$  and  $\mathcal{H}$  instead of functions  $F$  and  $H$ . The generalized Poisson bracket is given by

$$(23) \quad \{\mathcal{F}, \mathcal{G}\} = \int_0^h \left[ \left( \frac{\delta \mathcal{G}}{\delta w} \frac{\partial}{\partial z} \frac{\delta \mathcal{F}}{\delta \rho} - \frac{\delta \mathcal{F}}{\delta w} \frac{\partial}{\partial z} \frac{\delta \mathcal{G}}{\delta \rho} \right) + \frac{1}{\rho} \left( \frac{\delta \mathcal{F}}{\delta w} \frac{\delta \mathcal{G}}{\delta \theta} - \frac{\delta \mathcal{G}}{\delta w} \frac{\delta \mathcal{F}}{\delta \theta} \right) \frac{\partial \theta}{\partial z} \right] dz,$$

and the Hamiltonian energy functional is

$$(24) \quad \mathcal{H} = \int_0^h \left( \frac{1}{2} \rho w^2 + \rho U_i(\rho, \theta) + \rho g z \right) dz,$$

with internal energy  $U_i(\rho, \theta) = c_v T$  for an ideal gas; see Bokhove and Oliver (2006). To derive the equations of motion from (22)–(24) see Appendix Box 2.

By inspection,  $\{\mathcal{F}, \mathcal{H}\}$  is seen to be anti-symmetric, but the Jacobi identity

$$(25) \quad \{\mathcal{F}, \{\mathcal{G}, \mathcal{K}\}\} + \{\mathcal{G}, \{\mathcal{K}, \mathcal{F}\}\} + \{\mathcal{K}, \{\mathcal{F}, \mathcal{G}\}\} = 0,$$

for arbitrary functionals  $\mathcal{F}, \mathcal{G}$  and  $\mathcal{K}$ , is (in 3D) much more complicated to prove. However, by using the same transformation relations between the parcel functions and functionals that were used in finding (23), we can deduce that

$$(26) \quad \{\mathcal{F}, \{\mathcal{G}, \mathcal{K}\}\} = \int \{F, \{G, K\}\} dz,$$

where the functions  $F, G, K$  are associated with the functionals  $\mathcal{F}, \mathcal{G}, \mathcal{K}$  respectively. Since by (19) the Jacobi identity holds for the functions  $F, G, K$ , the Jacobi identity (25) for functionals follows immediately from (26). The above is the most straightforward derivation of the Hamiltonian formulation for the PDE system (corresponding to the parcel ODE system) known to us.

*Second*, a discretization preserving the Hamiltonian parcel formulation is available (Frank, Gottwald and Reich 2002). Consequently, the conservation laws in the continuum framework have discrete analogs, an important achievement. In fact, this discretization was discovered before the continuum parcel formulation (Bokhove and Oliver 2006) was recognized and linked to other Hamiltonian formulations. A discretization is obtained simply by putting indices  $k$  on (6) and approximating  $\Pi_e$ , thus following  $N$  particles each with a fixed mass, to obtain

$$(27a) \quad \frac{dZ_k}{dt} = \frac{\partial H_c}{\partial W_k} = W_k,$$

$$(27b) \quad \frac{dW_k}{dt} = - \frac{\partial H_c}{\partial Z} \Big|_{Z=Z_k} = - \Theta_k \frac{\partial \Pi_h}{\partial Z} \Big|_{Z=Z_k} - g,$$

$$(27c) \quad \frac{d\Theta_k}{dt} = 0$$

with Hamiltonian

$$(28) \quad H_c(Z, W_k, \Theta_k, t) = \frac{1}{2} W_k^2 + \Theta_k \Pi_h(Z) + g Z.$$

A particle-mesh or particle-finite-element method is obtained because an approximate Exner's function  $\Pi_h(z, t)$  is reconstructed throughout space either by approximating the density-weighted potential temperature integral (12) on a finite difference grid followed by an interpolation step (cf. Frank, Gottwald and Reich 2002), or by using a finite element method, yielding the value of density-weighted potential temperature everywhere in space (see [4]). Density can be approximated likewise by discretization of (13).

*Third*, certain asymptotic approximations remain entirely within the framework of the ODE's for an individual parcel, which is often more straightforward than performing asymptotics on the PDE's.

*Fourth*, certain (classical) fluid parcel instabilities in meteorology and fluid dynamics are more readily obtained from the ODE's for a distinguished fluid parcel than from the associated partial differential equations. We consider the static stability of an air parcel next. It is a classical example of a parcel stability in meteorology (see, e.g., Salmon 1998).

## 5. Static (in)stability of the atmosphere

When there is no flow then  $W = 0$  and the momentum equation (6b) is in hydrostatic balance

$$(29) \quad \theta_g(Z) \frac{\partial \Pi_e(Z)}{\partial Z} + g = 0.$$

Parcel oscillations are analyzed in a static atmosphere for a given parcel energy of the form  $H_c = \frac{1}{2} W^2 + \theta \Pi_e(Z) + g Z$ . The Exner function  $\Pi_e(Z) = c_p (p(Z)/p_r)^\kappa$  is now chosen with a potential temperature  $\Theta(0; A) = \theta_g(Z)$  such that it satisfies (29). We choose an initial condition such that  $Z(0) = Z_r$  and  $\Theta(0) = \theta_g(Z_r)$ . We linearize the vertical momentum equation (6b) with respect to  $Z$  around a reference vertical level  $Z_r$  such that  $Z = Z_r + Z'$ . To obtain an expression linear in  $Z'$ , we use (29) and

$$\frac{d^2 \Pi_e}{dZ^2} = \frac{g}{\theta_g^2} \frac{d\theta_g}{dZ}$$

as function of  $Z_r$ , in a Taylor expansion of the right-hand-side of the vertical moment equation (6b)

$$\Theta \frac{\partial \Pi_e}{\partial Z} + g = \theta_g(Z_r) \left( \frac{d\Pi_e}{dZ}(Z_r) + \frac{d^2 \Pi_e}{dZ^2}(Z_r) Z' \right) + g + O(Z'^2) = N^2 Z' + O(Z'^2),$$

in which the symbol  $O(Z'^2)$  denotes terms of second or higher order. Hence, the linearized vertical momentum equation becomes

$$(30) \quad \frac{d^2 Z'}{dt^2} = -N^2 Z',$$

where

$$(31) \quad N^2 = N^2(Z_r) = (g/\theta_g) (d\theta_g/dZ)|_{Z=Z_r}$$

is the square of the Brunt-Väisälä frequency. Note that  $N$  has the dimension of frequency, since  $g$  has dimension length over time squared and  $Z$  has length as dimension. From (30), we see that the linear stability of the flow depends on the sign of  $N^2$ , for

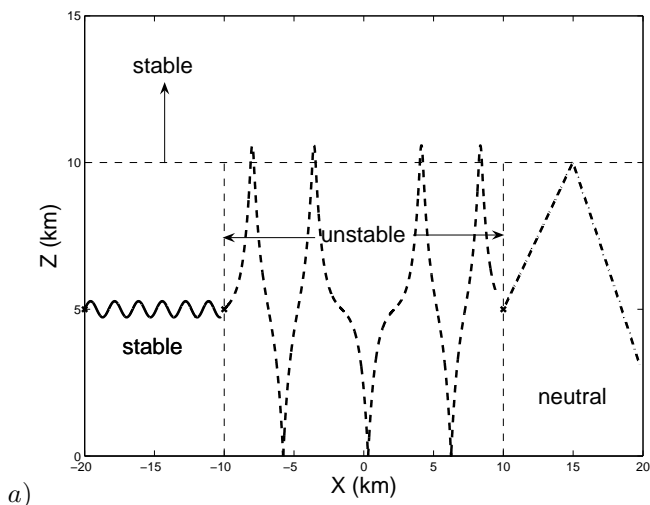
$$(32) \quad N^2 \begin{cases} > 0 & \text{the atmosphere is statically stable,} \\ = 0 & \text{statically neutral, and} \\ < 0 & \text{statically unstable.} \end{cases}$$

Hence, (30) results in stable harmonic oscillations of an air parcel around the reference level  $Z_r$  when  $N^2 > 0$ , a neutrally stable situation for  $N^2 = 0$ , and an unstable (exponentially growing) solution when  $N^2 < 0$ .

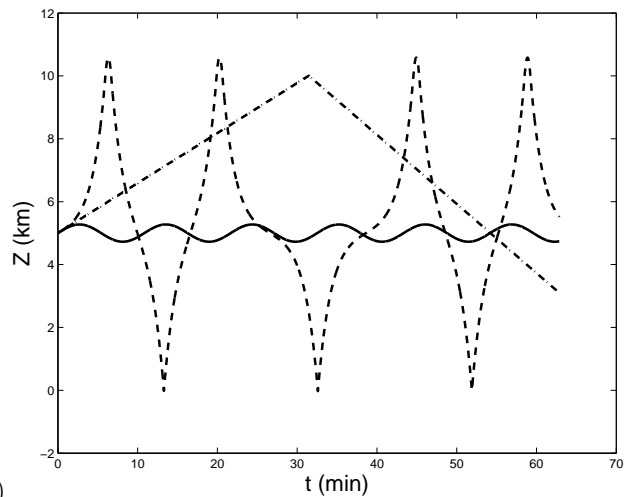
This linear behaviour explains the three idealized non-linear numerical simulations depicted in Fig. 3 for a given “hydrostatic” Hamiltonian

$$(33) \quad H_c = U^2/2 + W^2/2 + \Theta \Pi_e(Z) + gZ.$$

This Hamiltonian is called hydrostatic because we specify its potentials to satisfy (29) rather than determine the pressure from the (discrete collection of) air parcels. Also, the  $x$ -direction has been included for display purposes but the potential is  $X$ -independent such that  $dX/dt = U$  and  $dU/dt = 0$ . The  $X$ - $Z$ -plane is divided in four parts (thin dashed lines in Fig. 3a). We choose  $Z(0)$  and calculate  $\Theta(0) = \theta_g(Z(0))$ . In the stratosphere, above 10km, the basic atmosphere is stably stratified,  $N^2 > 0$ . In the troposphere, below 10km, we assume that the potential temperature of the basic atmosphere varies linearly with height. For  $X < -10$ km (and  $Z < 10$ km), it is stably stratified, with  $\theta_g = \theta_0 + \alpha Z$ , since then  $N^2 = g\alpha/(\theta_0 + \alpha Z) > 0$  using (31). For  $-10$ km  $< X < 10$ km, it is unstably stratified with  $\theta_g = \theta_0 - \alpha Z$ , since then  $N^2 = -g\alpha/(\theta_0 - \alpha Z) < 0$ . And for  $X > 10$ km, it is neutral,  $\theta_g = \theta_0$  and  $N^2 = 0$ .



a)



b)

Fig. 3. Stable and unstable fluid particle trajectories are shown for statically stable oscillatory flow (solid thick line), unstable flow (dashed thick line), and neutral flow (dashed-dotted thick line). These are numerical solutions of (6) using static Hamiltonian (33). Particle trajectories are shown (a) in a vertical cross section, and (b) as function of vertical position and time.

When  $W(0) = 0$ , no vertical movement occurs as hydrostatic balance holds in the vertical momentum equation. Instead, we specify  $W(0) \neq 0$ , and also  $U(0) > 0$ . In our set-up the parcel’s horizontal velocity remains constant. The initial position of a particle is denoted on the left of each trajectory with a “ $\times$ ”-symbol, at  $Z = 5$ km and  $X = -20, -10, 10$ km, respectively. Hence, we see in Fig. 3 that a (weakly nonlinear) particle trajectory (thick solid lines) in the stable troposphere displays approximately harmonic oscillations with a period of  $2\pi/N = 10.6$ min (see Fig. 3b). The potential temperature remains constant:  $\Theta(t) = \theta_g(Z(0))$ .

Once a particle is displaced to a vertical level, the particle would only remain in hydrostatic balance when it has a potential temperature  $\theta_g(Z)$  in accordance with the Exner function  $\Pi_e(Z)$  at that level. Since  $\Theta(t)$  is conserved and thus constant, the particle motion adjusts itself in the stable case to oscillatory motion. In the unstable case, the trajectory departs to the stably-stratified stratosphere where its velocity diminishes and the trajectory reverses smoothly (thick dashed lines). At the Earth’s surface, the particle is reflected. In the neutral case, a particle maintains its initial upward velocity until it reaches the stratosphere (thick dashed-dotted lines).

## 6. Final remarks

The Hamiltonian particle-mesh or particle-finite-element method outlined will be tested further in idealized climate simulations with weak forcing and dissipation. The equations of motion used in atmospheric climate simulations

are Hamiltonian in the absence of forcing and dissipation. In that limit, the essential and complicated nonlinearities are maintained. The question under investigation is whether the discrete preservation of the Hamiltonian formulation with its associated conservation properties remains important when (weak) forcing and dissipation are added. This investigation is motivated by preliminary results in low-dimensional models suggesting that this preservation of the Hamiltonian structure on the discrete level is important even in the presence of forcing and dissipation (Hairer *et al.* 2006).

Jason Frank's (CWI, Amsterdam) and Bob Peeter's (Twente) constructive criticism has been much appreciated. O.B. acknowledges a fellowship (2001–2006) from The Royal Netherlands Academy of Arts and Sciences (KNAW) during the course of this work. O.B. and P.L. are grateful for support from the Lorentz Center, Leiden.

### 7. Appendix Box 1: Ideal gas law

The ideal gas law states that the pressure  $p$  is proportional to the product of density  $\rho$  and temperature  $T$ , i.e.

$$(34) \quad p = R \rho T$$

with gas constant  $R$ . Using the first law of thermodynamics

$$(35) \quad T ds = c_p dT - \frac{1}{\rho} dp,$$

with entropy  $s$  and  $c_p$  ( $c_v$ ) the constant specific heat at constant pressure (volume), in combination with the ideal gas law allows us to rewrite temperature in terms of potential temperature  $\theta$  and pressure as follows

$$(36) \quad T = \theta (p/p_r)^\kappa.$$

Here we have introduced a constant reference pressure  $p_r$ ,  $\kappa = R/c_p$  and potential temperature

$$(37) \quad \theta = T_r e^{(s-s_r)/c_p},$$

with  $T_r$  and  $s_r$  integration constants arising in solving (35). From (37) we note that potential temperature  $\theta$ , commonly used in meteorology, and entropy  $s$  are closely related. For air  $R = c_p - c_v = 287\text{J}/(\text{kg K})$ ,  $c_p = 1004\text{J}/(\text{kg K})$ ,  $\kappa = 2/7$  and  $p_r = 1000\text{mb}$ . We refer to Stanley (1971) for more thermodynamics.

### 8. Appendix Box 2: Eulerian equations arising from Hamiltonian dynamics

**Exercise:** Derive the Euler equations of motion (20) from (22)–(24). Functional derivatives are defined by

$$(38) \quad \delta \mathcal{H}[w, \rho, \theta] = \lim_{\epsilon \rightarrow 0} \frac{\mathcal{H}[w + \epsilon \delta w, \rho + \epsilon \delta \rho, \theta + \epsilon \delta \theta] - \mathcal{H}[w, \rho, \theta]}{\epsilon}.$$

Together with the definition of the first deviation of the Hamiltonian

$$(39) \quad \delta \mathcal{H} \equiv \int_0^h \frac{\delta \mathcal{H}}{\delta w} \delta w + \frac{\delta \mathcal{H}}{\delta \rho} \delta \rho + \frac{\delta \mathcal{H}}{\delta \theta} \delta \theta dz$$

we can find the functional derivatives  $\delta \mathcal{H}/\delta w$  and so forth. Here we use the expressions in Appendix Box 1 to express the (derivatives of the) internal energy  $U_i = c_v T$  in the Hamiltonian (24) terms of  $\theta$  and  $\rho$ . In addition, the following trick

$$(40) \quad w(z, t) = \int_0^h w(z', t) \delta(z - z') dz'$$

is used again to write the function  $w(z, t)$  as a functional, thus we can take  $\mathcal{F} = w(z, t)$ , and likewise for the other variables.  $\square$

### 9. Appendix Box 3: Hamiltonian particle mesh method

We can discretize (6) for  $k = 1, \dots, N$  particles and then obtain (27) with Hamiltonian (28)<sup>2</sup>. The density and potential temperature integrals (13) and (12) are determined everywhere in the domain  $z \in [0, H]$  by using a finite element method instead of the finite difference method used in Frank, Gottwald and Reich (2002). We thus obtain finite element approximations  $\rho_h(z, t)$  and  $\theta_h(z, t)$  for  $\rho(z, t)$  and  $\theta(z, t)$ . An approximate pressure  $p_h(z, t)$  is subsequently found everywhere by using these  $\rho_h(z, t)$  and  $\theta_h(z, t)$  (properly projected) in (8).

The domain is tessellated with  $N_e$  finite elements  $K_k$ . Generally, the number of particles  $N$  used is taken much larger,  $N \gg N_e$ . Weak formulations for  $\theta$  and  $\rho$  are obtained by multiplication of  $q = \rho \theta$  and integral relations (12) and (13) with test functions  $v_0(z)$ ,  $v_1(z)$ , and  $v_2(z)$ , taken continuous only within an element  $K_k$  but continuous across elements, followed by integration over an element (only continuity  $C^0$  of test and basis functions is required). We obtain

$$(41) \quad \int_0^h v_0(z) q(z, t) dz = \int_{K_k} v_0(z) \rho(z, t) \theta(z, t) dz$$

$$(42) \quad \int_0^h v_1(z) q(z, t) dz = \int_0^h \int_0^{A_h} v_1(z) \rho_0(A) \Theta_0(A) \delta(z - z(t; A)) dz dA = \int_0^{A_h} v_1(Z(t; A)) \rho_0(A) \Theta_0(A) dA$$

$$(43) \quad \int_0^h v_2(z) \rho(z, t) dz = \int_0^h \int_0^{A_h} v_2(z) \rho_0(A) \delta(z - z(t; A)) dz dA = \int_0^{A_h} v_2(Z(t; A)) \rho_0(A) dA$$

<sup>2</sup>Appendix Box 3 is *not* part of the submission to *Nieuw Archief voor Wiskunde* but the additional appendix in [4].



The product  $q = \rho\theta$  is introduced explicitly so that if we keep  $\rho \geq 0$  numerically then  $q$  behaves appropriately as well. Otherwise, negative densities could appear, or  $q$  could be nonzero while  $\rho$  is zero. We replace these test functions and the variables by their finite element approximations  $v_{0h}, v_{1h}, v_{2h}, \rho_h, \theta_h$  and  $q_h$ . The next step is then to replace the integrals over label space in (41)–(43) by a weighted summation over the particles, as follows

$$(44) \quad \int_0^{A_h} v_2(Z(t; A)) \rho_0(A) dA \approx \sum_{k=1}^N v_{2h}(Z_k) m_k$$

with  $m_k = \rho_0(A) \Delta A_k$  the mass distributed to each particle  $k$  initially at time  $t = 0$ , and  $\Theta_k$  the potential temperature for particle  $k$ . Putting matters together, we obtain from (41)–(43) the discretized weak formulations

$$(45) \quad \int_0^h v_{0h}(z) q_h(z, t) dz = \int_{K_k} v_{0h}(z) \rho_h(z, t) \theta_h(z, t) dz$$

$$(46) \quad \int_0^h v_{1h}(z) q_h(z, t) dz = \sum_{k=1}^N v_{1h}(Z_k) m_k \Theta_k$$

$$(47) \quad \int_0^h v_{2h}(z) \rho_h(z, t) dz = \sum_{k=1}^N v_{2h}(Z_k) m_k.$$

From the expressions (45)–(47), we deduce next that mass and mass weighted potential temperature are conserved pointwise, as in (14) and (15). The time derivative of (47) yields

$$(48) \quad \sum_{K_k} \frac{d}{dt} \int_{K_k} v_{2h}(z) \rho_h(z, t) dz = \frac{d}{dt} \int_0^h v_{2h}(z) \rho_h(z, t) dz =$$

$$\frac{d}{dt} \int_0^h \sum_{k=1}^N v_{2h}(z) \delta(z - Z_k) m_k dz \iff$$

$$(49) \quad \int_0^h v_{2h}(z) \partial_t \rho_h(z, t) dz =$$

$$- \int_0^h \sum_{k=1}^N v_{2h}(z) \partial_z \delta(z - Z_k) W_k m_k dz =$$

$$- \int_0^h v_{2h}(z) \partial_z \left( \sum_{k=1}^N \delta(z - Z_k) W_k m_k \right) dz.$$

Equating the left and right hand-sides gives (14) provided we define the mass-weighted velocity

$$(50) \quad \rho_h(z, t) w_h(z, t) = \sum_{k=1}^N \delta(z - Z_k) m_k W_k$$

or preferably its weak formulation

$$(51) \quad \int_0^h v_{3h}(z) \rho_h(z, t) w_h(z, t) dz = \sum_{k=1}^N v_{3h}(Z_k) m_k W_k$$

involving another test function  $v_{3h}(z)$ . Conservation of mass-weighted potential temperature is proven likewise.

The finite element approach seems to be a flexible way to derive the overall discrete energy function since its basis in weak formulations allows us to largely follow the continuous derivations. We multiply (27b) by  $m_k W_k$  and sum over all particles  $k$  to obtain

$$(52) \quad \begin{aligned} & \sum_{k=1}^N \frac{d}{dt} \left( \frac{1}{2} m_k W_k^2 \right) = - \sum_{k=1}^N m_k \frac{dZ_k}{dt} \frac{\partial H_c}{\partial Z} \Big|_{Z=Z_k} \\ & = - \sum_{k=1}^N m_k \frac{dZ_k}{dt} \left( \Theta_k \partial_z \Pi_h(p(z, t)) + \partial_z \Phi_h(z) \right) \Big|_{z=Z_k} \\ & = - \int_0^h \partial_z \Pi_h \sum_{k=1}^N m_k W_k \delta(z - Z_k) \Theta_k + \\ & \quad \partial_z \Phi_h \sum_{k=1}^N m_k W_k \delta(z - Z_k) dz \\ & = - \int_0^h \rho_h(z, t) w_h(z, t) \theta_h(z, t) \partial_z \Pi_h + \\ & \quad \rho_h(z, t) w_h(z, t) \partial_z \Phi_h dz \\ & = \int_0^h \Pi_h \partial_z (\rho_h w_h \theta_h) + \Phi_h \partial_z (\rho_h w_h) dz \\ & = - \int_0^h \Phi_h \partial_t \rho_h + \Pi_h \partial_t (\rho_h \theta_h) dz \\ & = - \int_0^h \frac{\delta \mathcal{H}_h(w_h = 0)}{\delta \rho_h} \partial_t \rho_h + \frac{\delta \mathcal{H}_h(w_h = 0)}{\delta (\rho_h \theta_h)} \partial_t (\rho_h \theta_h) dz \\ & = - \frac{d}{dt} \int_0^h \rho_h (U_{ih} + \Phi_h) dz \end{aligned}$$

with potential  $\Phi = \Phi(z) = g z$ ,  $\rho_h w_h = \sum_{k=1}^N m_k \delta(z - Z_k) W_k$  and  $\rho_h w_h \theta_h = \sum_{k=1}^N m_k \delta(z - Z_k) W_k \Theta_k$ . We also used a variation on the first law of thermodynamics (35) to introduce the internal energy  $U_i$ :  $T ds = dU_i + p d(1/\rho)$  (e.g., Stanley 1971). Finally, the discrete energy follows from (52) as

$$(53) \quad H_{cd} = \sum_{k=1}^N \frac{1}{2} m_k W_k^2 + \int_0^h \rho_h (U_{ih} + \Phi_h) dz.$$

A system of algebraic equations is obtained by expansion of the test functions and variables into a finite number of basis functions. We choose a continuous Galerkin finite element basis for test and basis functions seredipity elements and functions in element  $K_k$ . Consequently, the expansions of the variables are continuous from one element to the other but not their derivatives. As usual in finite element methods, we map each element  $K_k$  with  $z = [z_k, z_{k+1}]$  and nodes  $z_k$  and  $z_{k+1}$  to a reference element  $\zeta = [-1, 1]$  with local coordinate  $\zeta$ . The mapping  $z = F_{K_k}(\zeta)$  in element  $K_k$  between these  $z$  and  $\zeta$  coordinates is linear. The basis functions chosen are the

serendipity functions in the reference frame. For order one,  $N_p = 2$  and

$$(54) \quad \begin{aligned} \psi_1(z) &= \frac{1}{2}(1 - \zeta) \\ \psi_2(z) &= \frac{1}{2}(1 + \zeta) \end{aligned}$$

for nodes  $\zeta = -1, 1$ . For order two,  $N_p = 3$  and

$$(55) \quad \begin{aligned} \psi_1(z) &= -\frac{1}{2}(1 - \zeta)\zeta \\ \psi_2(z) &= \frac{1}{2}(1 + \zeta)\zeta \\ \psi_3(z) &= (1 - \zeta^2) \end{aligned}$$

for nodes  $\zeta = -1, 1, 0$ . For order two,  $N_p = 4$  and

$$(56) \quad \begin{aligned} \psi_1(z) &= \frac{1}{16}(1 - \zeta)(9\zeta^2 - 1) \\ \psi_2(z) &= \frac{1}{16}(1 + \zeta)(9\zeta^2 - 1) \\ \psi_3(z) &= \frac{9}{32}(1 - \zeta^2)(1 - 3\zeta) \\ \psi_4(z) &= \frac{9}{32}(1 - \zeta^2)(1 + 3\zeta) \end{aligned}$$

for nodes  $\zeta = -1, 1, -1/3, 1/3$ . Note that these functions are chosen such that on the home node they are one and zero on the remaining nodes.

We expand the variables in  $N_n = N_p N_e$  of these polynomials as

$$(57) \quad \rho_h(z, t) = \sum_{l=1}^{N_n} \hat{\rho}_l(t) \psi_l(z)$$

with  $\hat{\rho}_l(t)$  the time dependent expansion coefficients, and likewise we have coefficients  $\hat{q}_l(t)$  and  $\hat{\theta}_l(t)$  for the other variables. Substituting these expansions and choosing  $\psi_m$  for all  $m = 1, \dots, N_p$  in turn for the arbitrary test functions in (45)–(47) yield algebraic equations for these coefficients  $\hat{\rho}_l(t)$ ,  $\hat{q}_l(t)$  and  $\hat{\theta}_l(t)$  per element. These can be solved, globally, on the nodes. Once these coefficients are determined, we can reconstruct  $\rho_h(z, t)$ ,  $\theta_h(z, t)$  and  $q_h(z, t)$  everywhere in space, cf. (57). Subsequently,  $\Pi_h(z, t)$  can be determined through (52) whence we can move the particles in time following (27). With a Störmer-Verlet second-order temporal discretization of (27), that is,

$$(58a) \quad Z_k^{n+1/2} = Z_k^n + \frac{\Delta t}{2} W_k^n$$

$$(58b) \quad W_k^{n+1} = W_k^n - \Delta t \left( \frac{\partial H_c}{\partial Z} \right) \Big|_{Z=Z_k^{n+1/2}}$$

$$(58c) \quad Z_k^{n+1} = Z_k^{n+1/2} + \frac{\Delta t}{2} W_k^n,$$

the phase space structure of the Hamiltonian particle dynamics is preserved; the dynamics are then expected to only display small-amplitude oscillations around the total energy of the discrete system (Hairer *et al.* 2006; Frank *et al.* 2002). The above novel Hamiltonian particle finite element method is currently implemented and tested.

In the finite element discretization, the functional derivatives of the discretized Hamiltonian and in particular the functional derivative with respect to  $\rho_h \theta_h$  must project onto the finite element space

$$(59) \quad \delta \mathcal{H}_h = \int_0^h \frac{\delta \mathcal{H}_h}{\delta(\rho_h w_h)} \delta(\rho_h w_h) + \frac{\delta \mathcal{H}_h}{\delta(\rho_h \theta_h)} \delta(\rho_h \theta_h) + \frac{\delta \mathcal{H}_h}{\delta(\rho_h)} \delta(\rho_h) dz.$$

Consequently  $\delta \mathcal{H}_h / \delta(\rho_h \theta_h) = \Pi_h = \tilde{\Pi}_m \psi_m$ . To obtain the  $\Pi_h(z, t)$  present in the parcel Hamiltonian, we use (46) and next the weak formulation

$$(60) \quad \int_0^h v_{4h}(z) \Pi_h(z, t) dz = \int_0^h v_{4h}(z) C_r \left( \frac{1}{q_h(z, t)} \right)^{1/(\kappa-1)} dz$$

with prefactor

$$(61) \quad C_r = \frac{c_p p_r^{1/(\kappa-1)}}{p_r^\kappa R^{1/(\kappa-1)}}.$$

The pseudo algorithm of the numerical discretization thus becomes:

Set parameters and arrays

Given initial condition  $\rho(z, 0), \theta(z, 0), w(z, 0)$ .

Use these to determine  $m_k$  and to

Initialize  $Z_k, W_k, \Theta_k$  for all particles  $k = 1, \dots, N$

Start time loop:

while ( $t_{ij} \leq T_{end}$ )

find time step  $\Delta t$

for all k:  $Z_k^{n+1/2} = Z_k^n + \frac{\Delta t}{2} W_k^n$

for all k: find node  $el(k)$

Determine “potential”  $\Pi_h(z, t)$  and its derivative

for all k:  $W_k^{n+1} = W_k^n - \Delta t \left( \frac{\partial \Pi_h(z, t)}{\partial z} \right) \Big|_{z=Z_k^{n+1/2}} + g$

for all k:  $Z_k^{n+1} = Z_k^{n+1/2} + \frac{\Delta t}{2} W_k^{n+1}$

$t_{ij} += \Delta t$

Do measurements?

## References

[1] D.K. Arrowsmith, and C.M Place, *Dynamical systems*, Chapman & Hall, 330 pp, 1992.

[2] O. Bokhove and M. Oliver, Parcel Eulerian-Lagrangian fluid dynamics of

rotating atmospheric flows, *Proc. R. Soc. A.* **462**, 2575–2592, 2006.

- [3] O. Bokhove and M. Oliver, Isentropic two-layer model for atmospheric dynamics, *Q. J. Royal Meteorological Society*, submitted, 2007.
- [4] O. Bokhove and P. Lynch, *Parcels and particles in meteorology with Hamiltonian particle mesh method*, Article with additional appendix, <http://eprints.eemcs.utwente.nl>, 2007. Posted online upon acceptance of the manuscript.
- [5] J. Frank, G. Gottwald and S. Reich, A Hamiltonian particle-mesh method for the rotating shallow-water equations, *Lecture Notes in Computational Science and Engineering*, **26**, 131–142, 2002.
- [6] E. Hairer, C. Lubich and G. Wanner, *Geometric numerical integration*, Springer, 644 pp., 2006.
- [7] J. Methven, *et al.*, Establishing Lagrangian connections between observations within air masses crossing the Atlantic during the ICARTT experiment, *J. Geophys. Res.*, **111**, D23S62, 2006.
- [8] L. F. Richardson, *Weather Prediction by Numerical Process*, Cambridge University Press, 236 pp. 1922. Reprinted with a new Introduction, 2006.
- [9] R. Salmon, *Lectures on geophysical fluid dynamics*, Oxford University Press, 192 pp., 1998.
- [10] H.E. Stanley, *Introduction to phase transitions and critical phenomena*, Oxford University Press, 308 pp. 1971.